2026 JULY 19–22 VANCOUVER, BC
JOINT AAPM | COMP MEETING

# Auto-segmentation of Cranial Nerves III to VIII in MRI CISS images

H. M. Lau[1], T. L. Chiu[1], S. K. Yu1[1]
[1]Medical Physics Department, Hong Kong Sanatorium & Hospital, Hong Kong

養和醫療
HKSH MEDICAL GROUP

## ABSTRACT

This study investigates a model for the automated segmentation of cranial nerves in the context of radiosurgery treatment planning for acoustic neuroma and trigeminal neuralgia. Current treatment planning systems are unable to perform automatic segmentation for cranial nerves, and the delineation of these small nerves often results in prolonged manual effort. This research aims to improve the efficiency of contour delineation for cranial nerves, particularly CN III to VIII, in MR CISS images by employing nnU-Net .

Eight retrospective 1.5T CISS MRI scans were retrieved from patients who underwent stereotactic radiosurgery for acoustic neuroma or trigeminal neuralgia. Cranial nerve regions CN III, IV, V, VI, and VII–VIII region were manually traced and contoured by a radiation oncologist. The images were cropped into volumes of 100 x 100 x 100 pixels, centred on the pons. The segmentation model was trained with nnU-Net using 3D full-resolution configuration and 5-fold cross-validation over 100 epochs.

The average Dice coefficients for the five structures (CN III, IV, V, VI, and VII–VIII region) in the training set reached 0.9 and above; however, performance for the testing set is lower, yielding coefficients of 0.47, 0.21, 0.64, 0.45, and 0.62 respectively. Corresponding mean surface distances measured are 2.12, 4.86, 0.40, 0.98, and 0.97 mm, indicating generally good positional accuracy.
The substantial discrepancy in performance between training and testing datasets can be attributed to different contour precision and extension across patients depending on individual SRS treatment objectives, as well as anatomical abnormality resulting from patient conditions.

This study successfully demonstrates automated segmentation of cranial nerves (CN III, IV, V, VI, VII-VIII region) in MR CISS images. Despite challenges due to limited sample size, small contour volume, and possible structural abnormality, the results demonstrated a good positional accuracy and visual agreement with manual contours, suggesting it to be a useful tool for enhancing treatment planning and evaluation efficiency after further development and validation.

## INTRODUCTION

This study investigates a model for the automated segmentation of cranial nerves in the context of radiosurgery treatment planning for acoustic neuroma and trigeminal neuralgia.

Current treatment planning systems are unable to perform automatic segmentation for cranial nerves, and the delineation of these small nerves often results in prolonged manual effort. This research aims to improve the efficiency of contour delineation for cranial nerves, particularly CN III to VIII, in MR CISS images by employing nnU-Net [1].

## METHODS AND MATERIALS

Eight retrospective 1.5T CISS MRI scans were retrieved from patients who underwent stereotactic radiosurgery for acoustic neuroma or trigeminal neuralgia. Cranial nerve regions CN III, IV, V, VI, and VII–VIII region were manually traced and contoured by a radiation oncologist. The images were cropped into volumes of 100 x 100 x 100 pixels, centred on the pons. The segmentation model was trained with nnU-Net using 3D full-resolution configuration and 5-fold cross-validation over 100 epochs.

## RESULTS & DISCUSSION

The average Dice coefficients for the five structures (CN III, IV, V, VI, and VII–VIII region) in the training set reached 0.9 and above; however, performance for the testing set is lower, yielding coefficients of 0.47, 0.21, 0.64, 0.45, and 0.62 respectively. Corresponding mean surface distances measured are 2.12, 4.86, 0.40, 0.98, and 0.97 mm, indicating generally good positional accuracy.

The substantial discrepancy in performance between training and testing datasets can be attributed to different contour precision and extension across patients depending on individual SRS treatment objectives, as well as anatomical abnormality resulting from patient conditions.

Table 1. Auto-segmentation result of the testing set

| | Dice coefficient | Hausdorff distance 95% percentile (HD95) (mm) | Mean surface distance (MSD) (mm) |
|---|---|---|---|
| CN III | 0.467 | 3.44 | 2.12 |
| CN IV | 0.206 | 13.11 | 4.86 |
| CN V | 0.640 | 1.59 | 0.40 |
| CN VI | 0.448 | 3.87 | 0.98 |
| CN VII-VIII region | 0.621 | 1.80 | 0.97 |

## REFERENCES

[1] Isensee, F., Jaeger, P. F., Kohl, S. A., Petersen, J., & Maier-Hein, K. H. (2021). nnU-Net: a self-configuring method for deep learning-based biomedical image segmentation. Nature methods, 18(2), 203-211.

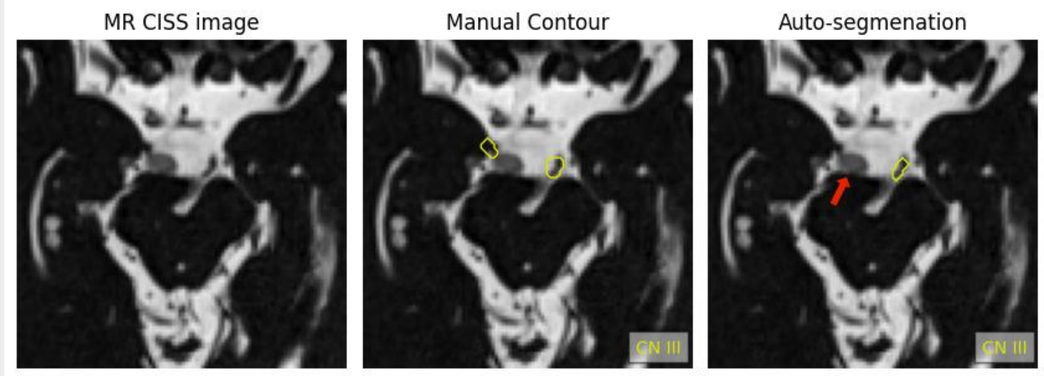


Figure 1. Auto- and manual segmentation performance of CN III (oculomotor nerve). The segmentation of the left CN III shows strong agreement with the manual contour regarding both position and volume. In contrast, the right CN III is affected by an abnormal structure (red arrow), which results in missed detection of the left CN III.

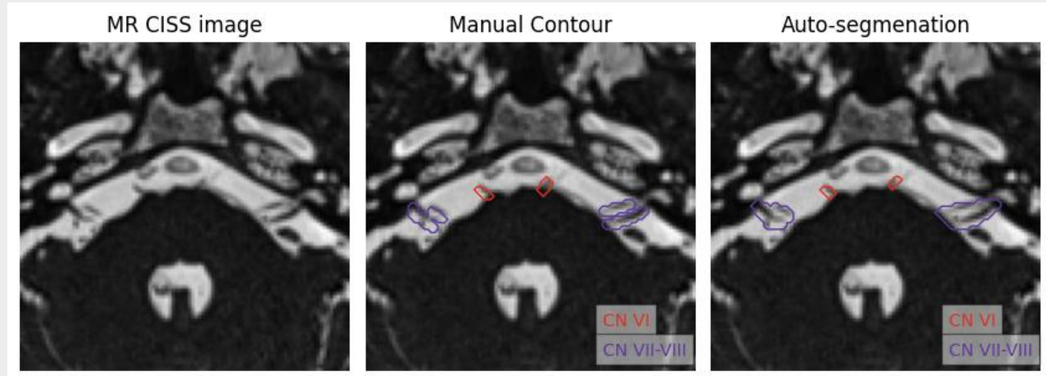


Figure 2. Auto- and manual segmentation of CN VI (abducens nerve), CN VII-VIII region (facial nerve and vestibulocochlear nerve). In regions with higher contrast, the automated segmentation closely aligns with the manual contours.

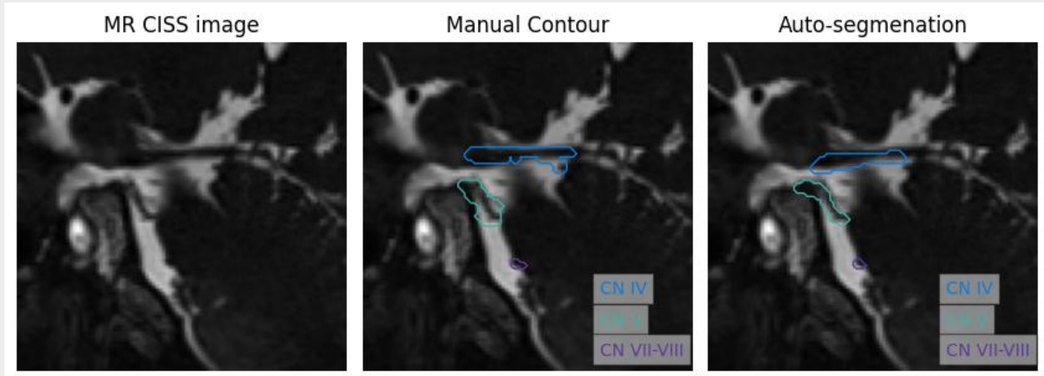


Figure 3. Sagittal view of auto- and manual segmentation of CN IV (trochlear nerve), CN V (trigeminal nerve) and CN VII-VIII region (facial nerve and vestibulocochlear nerve). CN IV exhibits the lowest Dice coefficient and largest surface distances among the five structures; this can be explained by its ambiguous extension and contrast nature in the image.

## CONCLUSIONS

This study successfully demonstrates automated segmentation of cranial nerves (CN III, IV, V, VI, VII-VIII region) in MR CISS images. Despite challenges due to limited sample size, small contour volume, and possible structural abnormality, the results demonstrated a good positional accuracy and visual agreement with manual contours, suggesting it to be a useful tool for enhancing treatment planning and evaluation efficiency after further development and validation.

© Poster Template by Genigraphics® 1.800.790.4001 www.genigraphics.com